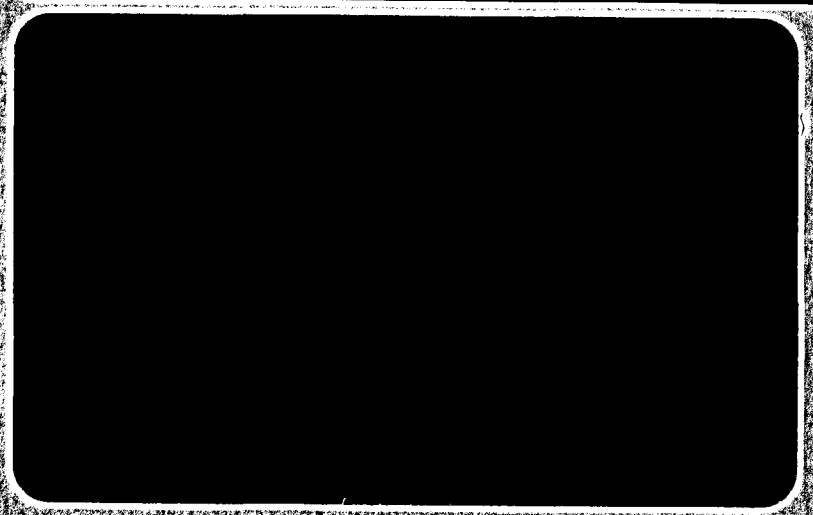

TU Delft
Delft University of Technology
Faculty of Aerospace Engineering

Memorandum M-819

Fractographic observations made in an exploratory test program on steel specimens loaded under constant-amplitude loading with intermediate batches of overload cycles

J. Schijve

11 November 1997

Fractographic observations made in an exploratory test program on steel specimens loaded under constant-amplitude loading with intermediate batches of overload cycles

J. Schijve

Abstract

Fatigue crack growth tests were carried out on low carbon steel specimens, thickness 4 mm. Load histories were used with periodic batches of OL cycles. The number of OL cycles in a batch as well as the number of base line cycles between the OL batches were varied. Fractographic observations in the SEM gave useful information on crack growth retardation, which can not be derived from ordinary crack growth records. The observations were base on the bands produced by the OL cycles. Striations were observed occasionally, but not as abundant as in Al-alloys. On a micro level the fatigue fracture surface is rather tortuous.

Symbols:

CA	Constant-Amplitude
VA	Variable-Amplitude
a	crack length
da/dN	crack rate
ΔK	stress intensity factor range
OL	overload

Introduction

The Faculty of Mechanical Engineering and Robotics of the University of Mining and Metallurgy in Krakow is starting a research program on fatigue crack growth in structural carbon steel under Variable-Amplitude (VA) loading. It includes both fatigue crack growth tests and a prediction model for crack growth. Assistance for planning the research program and for testing procedures is given by the Structures and Materials Laboratory of the Faculty of Aerospace Engineering of the Delft University of Technology. In view of the cooperation some crack growth experiments on steel specimens were carried out in Delft. The main purpose of these tests was to see whether fractographic information of steel specimens can be instructive to study interaction effects occurring during fatigue crack growth under VA load histories.

Crack growth tests were carried out on four CCT specimens. The results are presented and discussed in this Memorandum. It is completed with a number of summarizing conclusions. The Memorandum was primarily written for documentation of the experimental experience, and more in particular the fractographic evidence.

Acknowledgment: Jan Snijder, Bertil Grashof and Frans Oosterom have taken care of preparing specimens, programming the load histories, carrying out the fatigue tests, and making SEM pictures. The cooperation is greatly appreciated.

Survey of the experiments

Material

Low carbon steel was used because a plate was available in stock of the laboratory. The thickness of the plate was 4.0 mm. A chemical analysis indicated 0.7 % Mn and 1.1 % Si. The carbon content was estimated from the amount of pearlite. The estimate is 0.1 %.
Mechanical properties obtained in tensile tests were: lower σ_{yield} = 292 MPa, σ_{ult} = 433 MPa, elongation = 32 % (gage length 10 equivalent diameters = 80 mm). The tensile curve clearly indicated the typical low carbon yield behaviour.

Structure of the material

Microscopic samples were produced to reveal the material structure as seen on the L-LT plane, the L-ST plane and the LT-ST plane (L=longitudinal, LT=long transverse direction, ST=short transverse direction, see Fig.1). The samples were polished (final polish with 1μm diamond powder) and etched with Nital (Ethyl alcohol + nitric acid). Typical cross sections are shown in Figure 1. It shows a structure with fine equi-axed grains, and not a typical rolled pan cake structure. The grain diameter is in the order of 10 μm. Around midthickness slag streaks were observed, see Figure 2.

Crack growth specimens

The specimens width is W = 100 mm and the specimen thickness is t = 4 mm. The specimen dimensions are shown in Figure 3. The specimens were simply cut from an available plate, without any sheet surface machining or surface treatment. Because the quality of the sheet surface has a negligible effect on fatigue crack growth of through cracks, the most simple specimen production was supposed to be sufficient in view of the exploratory nature of the experiments.

The crack starter notch consists of a 3 mm hole with two hand made saw cuts at the two hole edges, leading to a crack starter notch, tip to tip about 10 mm (a_o = 5 mm).

Crack length measurements

Visual crack length measurements
In view of the exploratory nature of the tests a simple crack length measurement technique was adopted. A paper millimeter scale was attached to the specimen (Fig.3). The crack tip was observed through a binocular microscope with a low magnification (16x) at somewhat arbitrarily selected intervals.

Fractographic crack length measurements
Fracture surfaces of the three specimens tested under VA loading showed growth bands if the crack length was relatively large, in general exceeding 25 mm. In view of the correlation of these bands with the load spectrum, it allowed additional crack length measurements for large crack length, where the normal visual observations were missing.

Fatigue load histories

The three load histories of the three variable-amplitude experiments are shown in Figure 4. Each load spectrum is repeated until specimen failure. A spectrum consists of some sub-blocks with base line cycles and intermediate batches of overload (OL) cycles. They are programmed with the TestSTAR system. Unfortunately, in the second test an error was made which led to the an incorrect load history of little interest. The error was detected when the crack length was already $a \approx 10$ mm. The correct load history was then programmed to complete the test overnight, unattended. In the fourth experiment the specimen was tested under constant-amplitude loading ($S_{max} = 120$ MPa, $S_{min} = 7.5$ MPa).

Crack growth results

Visually obtained crack growth results are compiled in Tables 1 to 4. Graphs of the data are presented in Figures 5 to 9.

Specimen Steel-1

This specimen was tested under spectrum 1. Fig.5a shows the crack growth curve. Some irregularities can be observed. Unfortunately no crack length measurements were made for $a > 16$ mm. The crack growth rates (da/dN) in Fig.5c calculated from the visual crack growth records clearly confirm the irregularities of Fig.5a. The first and the last data points in Fig.5c are considered to be unreliable. It should be mentioned that it was not easy to accurately determine the location of the crack tip because of the unprepared specimen surface (as rolled, somewhat rusty scaling).

In order to eliminate the irregularities the crack growth records were "streamlined" by drawing (by hand) a smooth curve through the data and subsequently reading crack growth data from this curve, see Table 1b. As illustrated by Fig.5b and 5d the irregularities are then eliminated. Of course streamlining could also be done by a regression analysis of the data, or by omitting irregular a/N results of the records. It always should be questioned whether all data are sufficiently reliable for further analysis, which quite often is a matter of personal judgement. Apparently the very first a,N data of this test were not reliable (see Figs 5a and 5c). This could be due to the fact that the test was started with a lower stress level (S_{max} of OL=100 MPA). Crack nucleation did not occur, The stress level was then increased twice, first to S_{max}=125 MPa and finally to S_{max}=150MPa.

The fractographic growth results, derived from Figures 12 and 13 (see Table 1c) are included in Fig.5e. Although there is a large gap between the visual results and the fractographic results they could be very well in the same scatter band.

Specimen Steel-2

Due to the initially incorrectly programmed load history the first part of the crack growth record is invalid and can not be used. This was discovered when the crack length was about 10 mm. Rather than throwing the specimen away the operator decided to continue the test with the correct load history, i.e. spectrum 2 (Fig.4). This occurred during the night with no personal attendance and thus no visual crack growth observations. However, the fracture surface showed growth

bands (Fig.18) from which crack length measurements could be derived.

Results applying to the growth band corresponding to full spectrum blocks are presented in Table 2a and plotted in Fig.9. More refined measurements during the sub-blocks of the load spectrum were also possible. As shown by Fig.18 bands of the four batches of OL cycles of the full spectrum can be observed. The intervals between the OL cycle bands were measured from the fractographs with the SemAfore system. Because the crack extension during the OL cycle batches could not be measured accurately from the fractographs, the intervals Δa in table 2b include the crack extension during the OL cycles. It was then assumed that the crack rate during the 20 OL cycles was unaffected by the preceding base line cycles, and could thus be deduced from the Paris relation obtained in the CA test (Specimen Steel-4) as given in Eq(1). The crack extension of the base line cycle sub-block is corrected to $\Delta a - 20*(da/dN)_{OL}$. Crack rates for the base line cycles thus obtained are presented in Table 2b and plotted in Fig.6. The correction is rather small, in the order of a few to some 12%.

Specimen Steel-3

The specimen surface was hand polished with emery paper to improve the visibility of the crack tip. Crack growth records are presented in Table 3. The crack growth curve in Fig.7a shows a fairly smooth curve, but the crack rate in Fig.7b still shows some irregularities in the beginning of the test. By leaving out three data pairs (a,N), compare Table 3a with Table 3b, a more continuous da/dN-a relation is obtained, see Fig.7c. This is just another way of streamlining the crack growth records. The fractographic results derived from Fig.20 for the full spectrum blocks (four data points) are presented in Table 3c and plotted in Fig.7c. They appear to line up nicely with the growth rates of the crack growth records.

Bands of the batches of 50 OL cycles could again be used to derive the crack rate during the sub-blocks of base line cycles, in a similar way as described for specimen Steel-2. The results are presented in Table 3d and plotted in Fig.7d.

Specimen Steel-4

This specimen was tested under constant-amplitude loading: $S_{max} = 120$ MPa and $S_{min} = 7.5$ MPa, $R = 0.0625$). The plate surface was locally hand polished to facilitate crack tip location observations. The results are presented in Table 4 (streamlined data) and plotted in Figure 8. The crack growth curves (Fig.8a) suggest a continuous crack growth. The crack rate in Fig.8b initially shows small irregularities, which are considered to be due to inaccuracies of the crack length measurements and small Δa values between successive crack length observations. Leaving out a number of a,N data improves the crack growth rate curve (Fig.8c). These results are plotted in Fig.9 as a function of ΔK. The results follow the Paris relation quite nicely with a slope factor of 3.43. The Paris relation becomes:

$$\frac{da}{dN} = 1.38 * 10^{-6} * \Delta K^{3.43} \qquad (1)$$

(da/dN in mm/kc or μm/cycle, ΔK in MPA$\sqrt{m}$)

Fractography

Macroscopic fractography

The fatigue crack surfaces as examined by the naked eye show a relatively flat fracture surface, which is a characteristic feature for a fatigue crack. Initially the fracture surface was perpendicular to the loading direction, see Fig.10. There was a tendency to develop shear lips, but not as clear as usually observed for Al-alloys. At larger crack lengths shear lips became more evident. It could lead to a single shear fracture surface, but a double shear fracture was also observed. The final failure was a typical ductile failure with clear shear lips and necking.

Specimens 1, 2 and 3, loaded with the spectra with OL cycles, show macroscopic growth bands when the crack length was about 25 mm and larger, see Figure 10b. At those larger crack lengths the unbroken ligaments show indications of net section yielding and rumpling of the specimen surface. The surface of specimens Steel-3 and Steel-4 were hand polished. In the net section yield part the surface shows lines which are believed to be Lüderbands, see Fig.11 for a schematic picture. The bands are not easily documented with photos. The Lüderbands occur in the typical triangle also observed in the final failure area of Al-alloy sheet specimens tested for residual strength. The length of the triangle, ℓ in Fig.11, was about about 24 mm for specimen Steel-3 and about 21 mm for specimen Steel-4. At those values the net section stress at S_{max} of the experiment (150 and 120 MPA respectively) is 312 MPA and 286 MPA for the two specimens respectively. Both stress levels are close to the lower yield stress of 292 MPA. Another noteworthy observation then is that the bands of the OL cycles were only visible for crack length values above some 25 mm, i.e. when the specimen ligaments came into net section yield.

Fractographic observations in the SEM

The observations in the electron microscope indicate that the fracture surfaces on a micro level are not flat at all. Typical illustrations at small to moderate magnifications are shown in Figures 12 to 14. At larger magnifications the fracture surfaces are quite rough with a tortuous topography, see Figures 15-17, 19 and 22-24. It may be that the tortuous crack growth is associated with the presence of pearlite isles, which can be local barriers to cyclic slip and crack extension.

The bands of the OL cycles, already visible with the naked eye (Fig.10b), are clearly visible in the SEM. Similarly to the macroscopic experience, these bands could not be observed in the SEM for crack length values up to a $\approx$ 25 mm. At larger crack lengths the SEM clearly showed such bands on all three specimens tested under variable-amplitude loading (Figs 12-14, 18, 20,20, 21). Specimen Steel-1 was alternately loaded with a single OL cycle and a batch of 10 OL cycles, with 100 smaller base line cycles in between. The bands of a batch of 10 OL cycles is broader and more easily observed than a band of a single OL-cycle, see Fig.12. In Figure 13 the single OL cycle bands can not be observed any more. Increasing the magnification was of little help. Larger magnifications of the OL cycle bands are shown in Figs 14 and 15. They illustrate again the tortuous appearance. At still larger magnifications striations could occasionally be observed, see Fig.16. The crack length for this figure (a = 27.2 mm) corresponds to an average crack rate of 0.8 μm/cycle (see Fig.5c). This value agrees more or less with the striation spacing in Fig.16. For that reason the lines in Fig.16 are believed to be striations of individual load cycles. Unfortunately they could not be observed at many places. A picture like Fig.16 was more an exception than a typical observation.

The picture in Fig.19 most probably shows striations of a batch of 20 OL cycles (spectrum 2), although not very nice striations. Recently well defined striations of batches of OL cycles and single OL cycles have been observed on fracture surfaces of Al-alloy specimens tested under similar load spectra. The results of that parallel test program will be published shortly.

Better striations of OL-cycles were observed on specimen Steel-3 tested with batches of 50 OL cycles (spectrum 3), see Fig.22. The striation spacing is about 1.5 μm/cycle, which is about 3 times the average crack growth rate (0.5 μm/cycle) according to Fig.7c. This might be expected because ΔK is 1.36 times larger than for the base line cycles. In the adjacent area of the OL cycles of Fig.22 faint lines, see Fig.23, could be striations of the base line cycles. The spacing of these lines appears to be of the same magnitude as the average 0.5 μm/cycle crack growth rate.

As shown by Figures 13, 18 and 20, the visibility of the OL cycle bands decreases for smaller cracks. For these smaller cracks it was still explored whether striations could be observed at large magnifications. Examples are given in Figures 17 and 24. Figure 17 shows lines, which are not really sharply defined. The spacing is in the order of 0.3-0.4 μm, whereas the crack rate at that crack length is about 0.045 μm/cycle. Most probably the lines in Fig.17 are not striations, although similar pictures could be obtained at other locations as well.

Figure 24 shows a different type of lines. Here the striation spacing agrees more or less with the applicable average crack rate of 0.06 μm/cycle. The lines are considered to be real striations.

Discussion

The results of all specimens have been plotted in Fig.9. The results can be divided in two groups, i.e. da/dN results for $\Delta K < 35 MPa\sqrt{m}$ and another group with $\Delta K > 35 MPa\sqrt{m}$. The first group corresponds to data obtained through visual crack growth measurements and the second group to data derived from fractographic observations. The first group according to Fig.9 shows a good agreement with the CA data, except for a few initial results of specimen Steel-1. The agreement implies that crack growth retardation did not occur for spectrum 1 and 3 in this ΔK region. It is possible that the difference between S_{max} of the OL cycles and S_{max} of the base line cycles was too small to obtain a noticeable crack growth retardation. The absence of a retardation does not mean that interaction effects did not occur. It is possible that accelerated crack growth during the OL cycles is compensated by retarded crack growth during the base line cycles.

For $\Delta K > 35 MPa\sqrt{m}$, or roughly a>25 mm, it is suggested by Fig.9 that some crack growth acceleration occurred, rather than retardation. Such an acceleration followed by delayed retardation was recently shown by Dougherty et al. [1] in experiments with a single OL on CT specimens of steel 1070M, a carbon steel with 0.68% C.

As pointed out before, the a>25 mm region is also associated with net section yield during S_{max} of the OL cycles. It implies that the 1st OL cycle of a batch of OL cycles causes significant crack tip plastic deformation. That may explain why the fractographic bands of the OL cycles are caused only during in the a>25 mm region. It is expected that this occurs especially during the 1st OL cycle of each batch of OL cycles in agreement with the primary plastic flow concept proposed by de Koning and Dougherty [2] (see also [3]).

The effect of the OL cycles on the crack growth during the base line cycles is illustrated by Figs. 6 and 7d for specimens Steel-2 and Steel-3 respectively. As a reference the crack rate

under CA crack growth is also given in these graphs. It suggests that crack growth acceleration occurs during all sub-blocks of the base line cycles. However, more acceleration occurs during the shorter sub-blocks. In the longest sub-blocks (800 cycles in Fig.6, 1000 cycles in Fig.7d) the acceleration is fairly limited. Actually, the various sub-blocks of spectrums 1, 2 and 3 (Fig.4) were applied in order to see whether different retardations would occur in these sub-blocks. However, acceleration has been found. The smaller acceleration for longer sub-blocks indicates a transient effect. Some interaction must thus have occurred. A description of the crack closure behaviour under the present net section yield condition is a matter of speculation. It is still expected that the primary plastic zone, created by the OL cycles, will decelerate crack growth into this zone during the subsequent base line cycles. That could still be a crack closure induced retardation. However, at the same time, it is possible that ΔK_{eff} is still larger than under CA loading because of the overall crack tip opening due to the occurrence of net section yield. If this picture is correct, it should be expected that the OL induced crack closure diminishes during an increasing number of base line cycles. And that was actually observed. In passing, it may be pointed out that the above phenomenon could be observed thanks to a fractographic fracture surface examination. The same observations can not be obtained from the usual macroscopic crack growth records.

Summarizing conclusions

Four fatigue crack growth tests were carried out on low carbon steel specimens of 4 mm thickness, width = 100 mm. Three different variable-amplitude load histories were used, consisting of constant-amplitude base line cycles and periodic overload cycles. The periodic OL cycles were applied as single OL cycles and as batches of OL cycles (10, 20 and 50). The number of base line cycles between the periodic OL cycles was also varied (values between 100 and 1000). The prime purpose was to explore the usefulness of fractographic observations to get more detailed information on crack growth under VA-loading. The experience is summarized below in a number of conclusions.

1. The fracture surfaces of the fatigue cracks are macroscopically rather flat as usual for fatigue failures. However, on a micro level the topography of the fracture surfaces is rough and tortuous.
2. For cracks up to about 25 mm the OL cycles did not induce crack growth retardation, probably as a consequence of a too small difference between S_{max} of the OL cycles and S_{max} of the base line cycles.
3. Bands of the OL cycles could be observed for relatively long cracks, but not for small cracks. The bands occurred when the uncracked ligaments came into net section yield. The OL bands could be observed with the unaided eye, but in much more detail in the SEM. The visibility of the bands was good for batches of OL cycles (10 to 50 in a batch), but much less for single OL cycle bands.
4. Average crack growth rates derived from the OL cycle bands were in good agreement with the results derived from the crack growth records of the visual observations during the fatigue tests.
5. Although the OL cycle bands could be observed for longer cracks only, they gave worthwhile information on transient crack growth interaction effects. Such detailed information can not be obtained from ordinary crack growth records. It indicated some crack growth acceleration immediately after the OL cycles. The acceleration decreased

after more base line cycles, but a retardation was not yet obtained.

6. Further experiments are necessary for a more complete picture of the delayed retardation phenomenon in this steel. A larger difference between S_{max} of the OL cycles and S_{max} of the base line cycles and larger batches of the base line cycles should be recommended.
7. Striations of the OL cycles and the base line cycles were occasionally obtained. However, striations in this low carbon steel are by far much less abundant and less clearly defined as they are for Al-alloys.

References

[1] Dougherty, J.D., Srivatsan, T.S. and Padovan, J., Fatigue crack propagation and closure behavior of modified 1070 steel: Experimental results. Engineering Fracture Mechanics, Vol.56, 1997, 167-187.

[2] de Koning,A.U. and Dougherty,D.J., Prediction of low and high crack growth rates under constant and variable amplitude loading. In: Fatigue crack growth under variable amplitude loading, (J.Petit et al., eds.), 1989, pp.208-217.

[3] Schijve,J., Fundamental aspects of predictions on fatigue crack growth under variable-amplitude loading. Theoretical Concepts and Numerical Analysis of Fatigue. Proc. Conf. 25-27 May, 1992, Un. of Birmingham (eds. A.F.Blom and C.J.Beevers). EMAS (1992), pp.111-130

Specimen Steel-1			
Cycles	left crack (mm)	right crack (mm)	average (mm)
0	5.0	5.2	5.1
10012	6.8	7.0	6.9
15100	6.8	7.2	7.0
20037	6.9	7.8	7.35
26519	7.5	7.9	7.7
30016	7.8	8.0	7.9
35041	8.0	8.1	8.05
40015	8.0	8.3	8.15
50004	8.8	9.0	8.9
65047	9.0	10.0	9.5
75290	9.8	10.0	9.9
85138	10.2	10.2	10.2
100020	11.0	11.0	11.0
120698	12.2	12.3	12.25
134431	13.1	13.5	13.3
139504	13.4	13.5	13.45
153216	15.0	15.0	15.0
163346	15.0	15.5	15.25
244385	specimen failure		

Table 1a: Crack growth records

Streamlined data				
a (mm)	N (kc)	a-average	da/dN mm/kc	ΔK MPA√m
7	13			
8	35	7.5	0.046	17.51
9	57	8.5	0.046	18.72
10	79	9.5	0.046	19.88
11	100	10.5	0.048	21.01
12	117	11.5	0.059	22.11
13	132	12.5	0.067	23.19
14	145	13.5	0.077	24.27
15	157	14.5	0.083	25.34
16	167	15.5	0.100	26.41

Table 1b: Streamlined records

crack rates derived from fractographic bands			
a(*) (mm)	a-av. (mm)	da/dN (mm/kc)	ΔK (MPa√m)
25.65			
25.79	25.72	0.65	38.47
25.91	25.85	0.58	38.65
26.05	25.98	0.65	38.83
26.19	26.12	0.69	39.03
26.33	26.26	0.65	39.23
26.45	26.39	0.54	39.41
26.60	26.52	0.71	39.60
26.77	26.68	0.82	39.83
26.91	26.84	0.69	40.06
27.07	26.99	0.75	40.28
27.26	27.17	0.91	40.54
27.43	27.35	0.81	40.81
27.62	27.53	0.87	41.07
27.80	27.71	0.85	41.34
28.02	27.91	1.03	41.65
28.19	28.10	0.82	41.95
28.39	28.29	0.98	42.24
28.61	28.50	1.01	42.57
28.83	28.72	1.05	42.92
29.07	28.95	1.13	43.29
29.31	29.19	1.15	43.68
29.62	29.46	1.46	44.14
29.90	29.76	1.34	44.64
30.21	30.06	1.48	45.15
30.60	30.40	1.81	45.75
31.02	30.81	2.00	46.47
31.56	31.29	2.59	47.37
32.30	31.93	3.48	48.59

(*) crack length values of fractographic bands of batches of 10 OL cycles.

Table 1c: Results derived from fractographic measurements in the SEM

Table 1: Crack growth data of specimen Steel-1

Specimen Steel-2, results of fractographic measurements (picture Steel-2-5)				
a (mm)	Δa (mm)	da/dN (mm/kc)	a-average (mm)	ΔK (MPA√m)
27.00				
27.86	0.86	0.54	27.43	40.9
28.87	1.01	0.64	28.36	42.4
30.13	1.26	0.80	29.50	44.2
31.70	1.57	0.99	30.92	46.7

(*) crack length value of fractographic bands of the first batch of 20 OL cycles.

Table 2a: Crack growth data of specimen Steel-2, obtained from fractographs for full spectrum blocks at large crack length.

Specimen Steel-2, results of fractographic measurements (picture Steel-2-5)						
block	sub-block	cycles in sub-block	Δa (mm)	da/dN (mm/kc)	a-average (mm)	ΔK (MPA√m)
1	1	100	0.088	0.79	26.84	40.06
	2	200	0.129	0.61	26.95	40.22
	3	400	0.226	0.54	27.13	40.48
	4	800	0.419	0.51	27.45	40.96
2	1	100	0.088	0.78	27.61	41.20
	2	200	0.138	0.64	27.73	41.38
	3	400	0.276	0.67	27.95	41.71
	4	800	0.507	0.61	28.34	42.32
3	1	100	0.115	1.04	28.65	42.81
	2	200	0.170	0.79	28.79	43.03
	3	400	0.318	0.77	29.04	43.44
	4	800	0.659	0.80	29.53	44.25
4	1	100	0.120	1.07	29.91	44.89
	2	200	0.235	1.11	30.09	45.20
	3	400	0.419	1.02	30.42	45.78
	4	800	0.793	0.97	31.03	46.88

Table 2b: Crack growth data of specimen Steel-2, obtained from fractographs for sub-blocks at large crack length.

Table 2: Crack growth data of specimen Steel-2

Specimen Steel-3							
cycles	a-left (mm)	a-right (mm)	a-av. (Mm)	dN	da (mm)	da/dN (mm/kc)	a (mm)
60135	5.8	5.1	5.45				
80124	6.0	5.8	5.90	19989	0.45	0.0225	5.68
110221	6.3	6.2	6.25	30097	0.35	0.0116	6.08
131133	6.8	6.4	6.60	20913	0.35	0.0167	6.43
150122	7.2	6.8	7.00	18989	0.40	0.0211	6.80
165345	7.4	7.0	7.20	15223	0.20	0.0131	7.10
193182	7.9	7.6	7.75	27837	0.55	0.0198	7.48
226947	8.8	8.6	8.70	33766	0.95	0.0281	8.23
246681	9.5	9.0	9.25	19734	0.55	0.0279	8.98
290963	10.8	10.6	10.70	44283	1.45	0.0327	9.98
342075	12.8	12.7	12.75	51112	2.05	0.0401	11.73
367449	14.4	14.1	14.25	25375	1.50	0.0591	13.50
390846	15.7	15.5	15.60	23397	1.35	0.0577	14.93
417721	17.8	18.3	18.05	26876	2.45	0.0912	16.83
434609	19.5	20.7	20.10	16888	2.05	0.1214	19.08
452968	23.0	25.3	24.15	18359	4.05	0.2206	22.13
462500	failure						

Table 3a: Crack growth records of specimen Steel-3

Specimen Steel-3, some data pairs left out						
N	a-average (mm)	ΔN	Δa (mm)	da/dN (mm/kc)	a (mm)	ΔK (MPA√m)
80124	5.90					
110221	6.25	30097	0.35	0.0116	6.08	14.38
150122	7.00	39902	0.75	0.0188	6.63	15.04
193182	7.75	43060	0.75	0.0174	7.38	15.91
226947	8.70	33766	0.95	0.0281	8.23	16.86
246681	9.25	19734	0.55	0.0279	8.98	17.67
290963	10.70	44283	1.45	0.0327	9.98	18.72
342075	12.75	51112	2.05	0.0401	11.73	20.49
367449	14.25	25375	1.50	0.0591	13.50	22.25
390846	15.60	23397	1.35	0.0577	14.93	23.64
417721	18.05	26876	2.45	0.0912	16.83	25.51
434609	20.10	16888	2.05	0.1214	19.08	27.78
452968	24.15	18359	4.05	0.2206	22.13	31.02

Table 3b: Specimen Steel-3, same data as in Table 3a, but some data pairs left out.

Specimen Steel-3, averages of full blocks		
a (mm)	ΔK (MPA√m)	da/dN (mm/kc)
25.3	34.74	0.42
26.1	35.75	0.43
27.0	36.93	0.49
28.0	38.31	0.64

Table 3c: Specimen Steel-3, average results obtained from fractographic pictures for full spectrum blocks.

Specimen Steel-3, results of fractographic measurements (picture Steel-3-2)						
block	sub-block	cycles in sub-block	Δa (mm)	da/dN (mm/kc)	a-average (mm)	ΔK (MPA√m)
1	1	250	0.153	0.57	25.15	34.55
	2	500	0.229	0.43	25.34	34.79
	3	1000	0.374	0.36	25.64	35.16
2	1	250	0.161	0.58	25.91	35.51
	2	500	0.256	0.48	26.12	35.78
	3	1000	0.416	0.40	26.46	36.22
3	1	250	0.161	0.58	26.74	36.59
	2	500	0.314	0.60	26.98	36.91
	3	1000	0.450	0.43	27.36	37.42
4	1	250	0.246	0.91	27.71	37.90
	2	500	0.331	0.62	28.00	38.31
	3	1000	0.576	0.56	28.45	38.95
5	1	250	0.374	1.42	28.93	39.66
	2	500	0.610	1.18	29.42	40.39

Table 3d: Crack growth data of specimen Steel-3, obtained from fractographs for sub-blocks at large crack length.

Table 3: Crack growth data of specimen Steel-3

Specimen Steel-4						
cycles	a-left (mm)	a-right (mm)	a-av. (mm)	a-mean (mm)	da/dN (mm/kc)	ΔK (MPa√m)
60784	5.9	5.6	5.75			
100008	6.6	6.4	6.50	6.13	0.019	15.75
140106	7.8	7.5	7.65	7.08	0.029	16.98
169997	8.5	8.3	8.40	8.03	0.025	18.15
200008	9.7	9.5	9.60	9.00	0.040	19.30
229999	11.0	10.9	10.95	10.28	0.045	20.76
244999	11.9	11.7	11.80	11.38	0.057	21.97
259999	12.8	12.6	12.70	12.25	0.060	22.92
274999	14.2	13.7	13.95	13.33	0.083	24.08
289999	15.5	15.0	15.25	14.60	0.087	25.44
304999	17.5	16.7	17.10	16.18	0.123	27.13
314999	19.0	17.9	18.45	17.78	0.135	28.87
324999	21.0	19.5	20.25	19.35	0.180	30.62
334999	23.5	21.4	22.45	21.35	0.220	32.92
340007	25.0	22.7	23.85	23.15	0.280	35.10
344999	26.8	24.2	25.50	24.68	0.331	37.06
350004	29.0	26.2	27.60	26.55	0.420	39.64
354999	32.5	29.5	31.00	29.30	0.681	43.87

Table 4: Crack growth records of specimen Steel-4 tested under CA loading.
S_{max} = 120 MPA, S_{min} = 7.5 MPA.

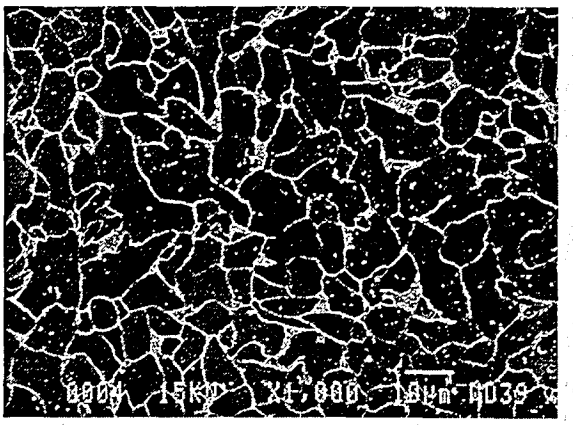

L-ST

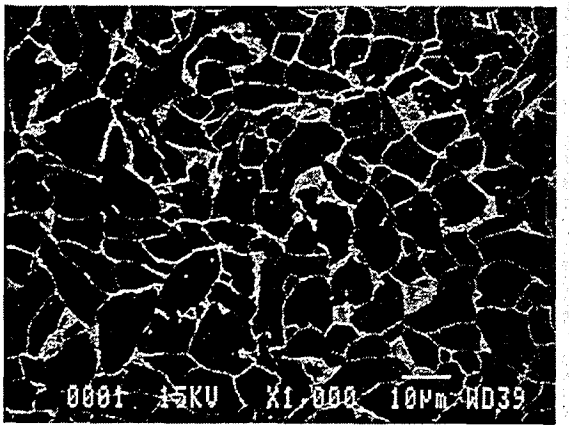

L-LT

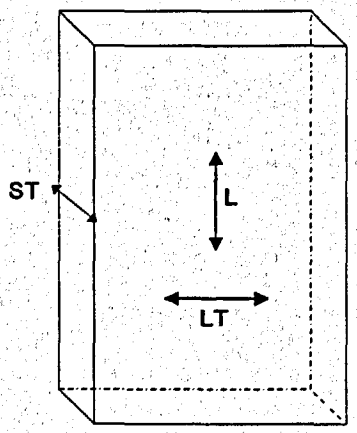

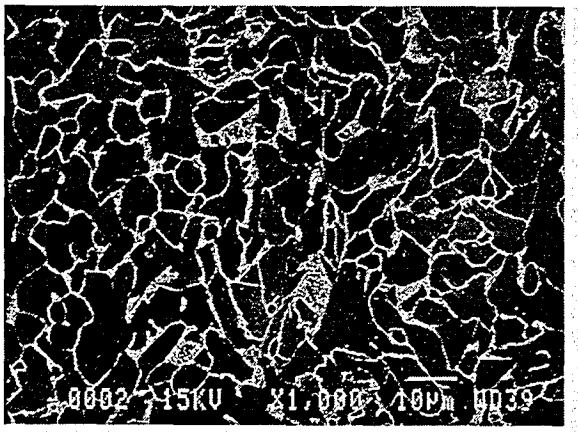

LT-ST

Fig.1: Equi-axed structure of steel.

L-ST cross section

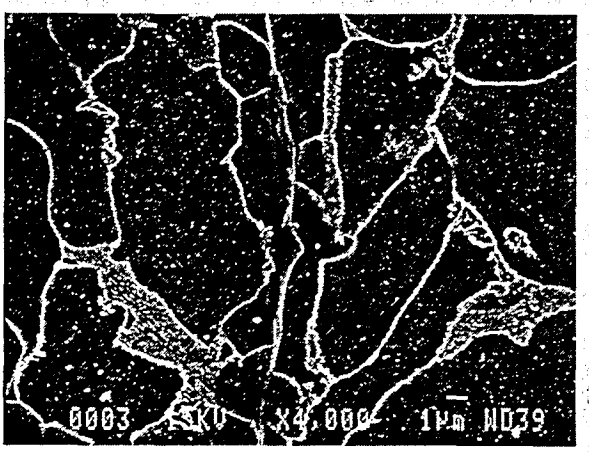

LT-ST cross section

Fig.2: The slag streaks at larger magnification.

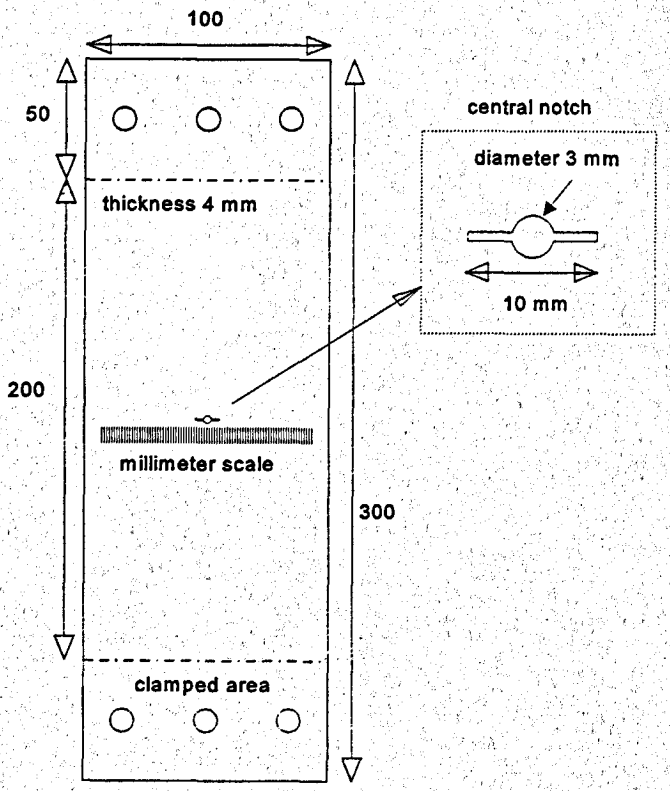

Fig.3: Center cracked tensile (CCT) specimen

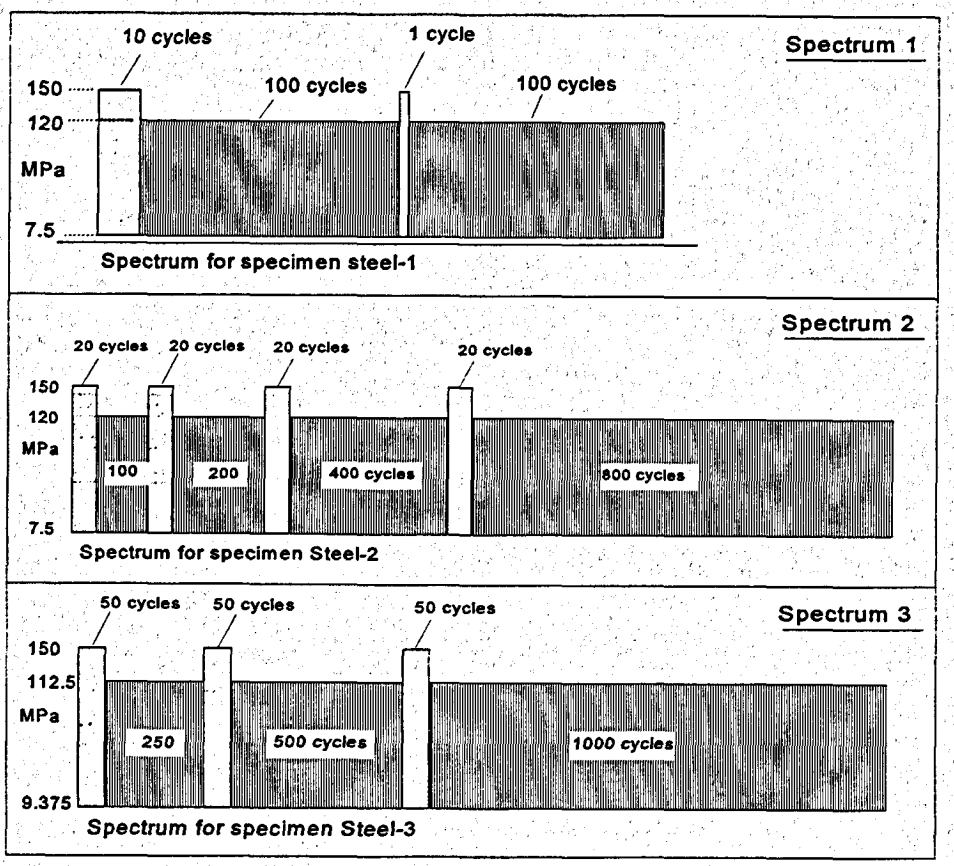

Fig.4: Load histories

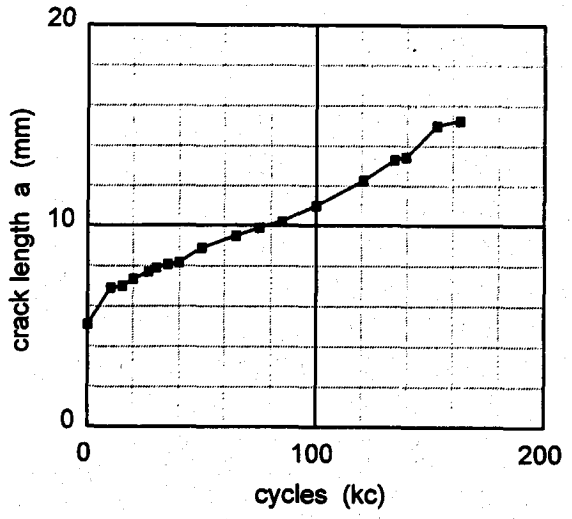

Fig.5a: Record of visual observations.

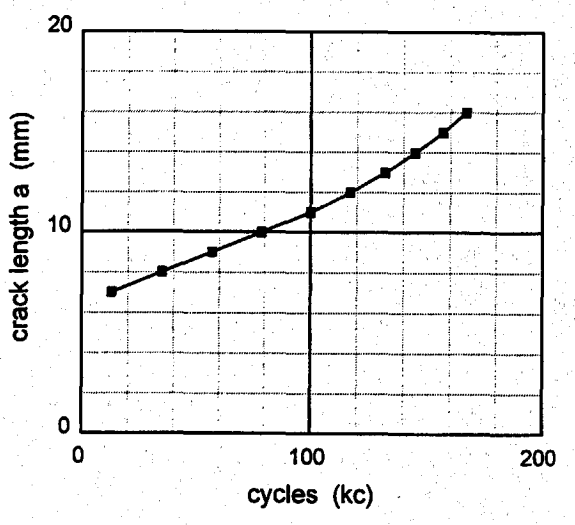

Fig.5b: Record of streamlined data.

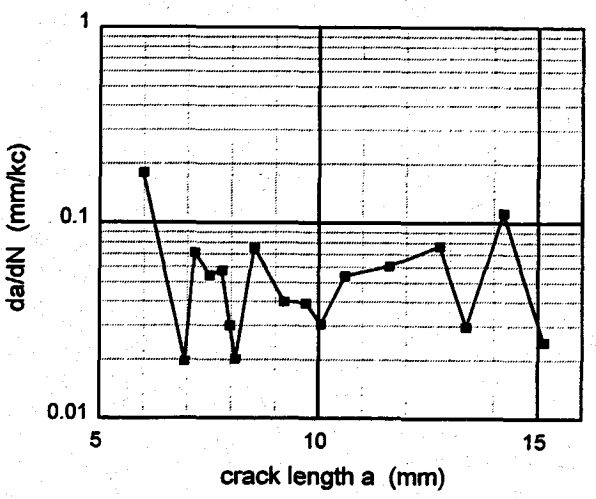

Fig.5c: Crack growth rates of the records.

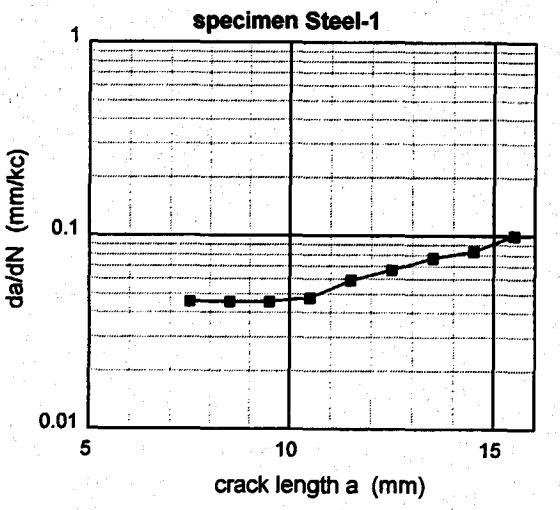

Fig.5d: Crack growth rates of streamlined data.

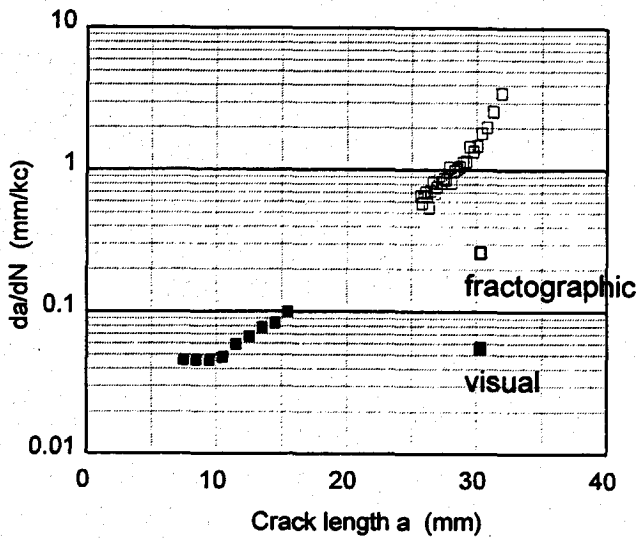

Fig.5e: Crack growth rates of visual and fractographic observations.

Fig.5: Results of specimen Steel-1.

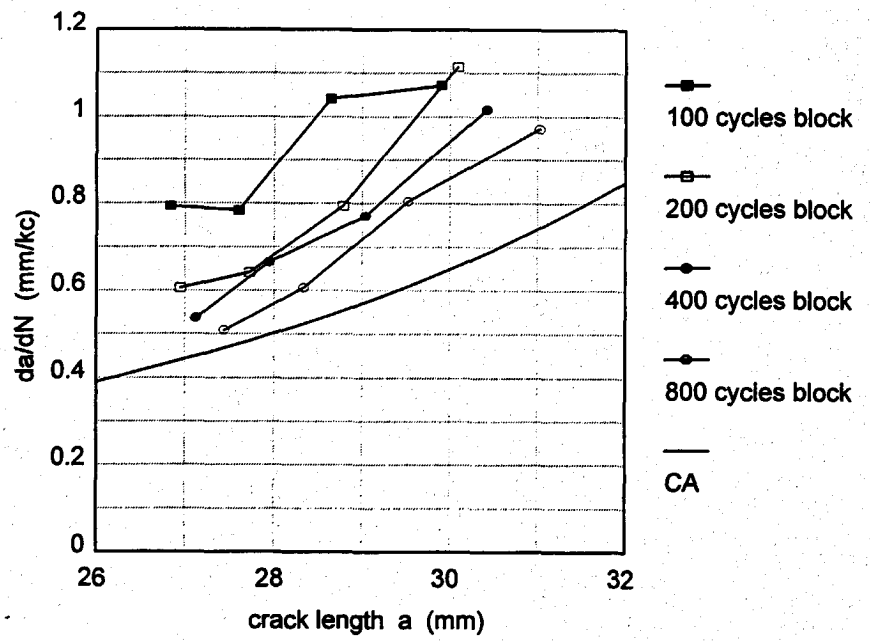

Figure 6: Specimen Steel-2. Crack growth rates in the four sub-blocks of spectrum 2. Results obtained from measurements on fractographs.

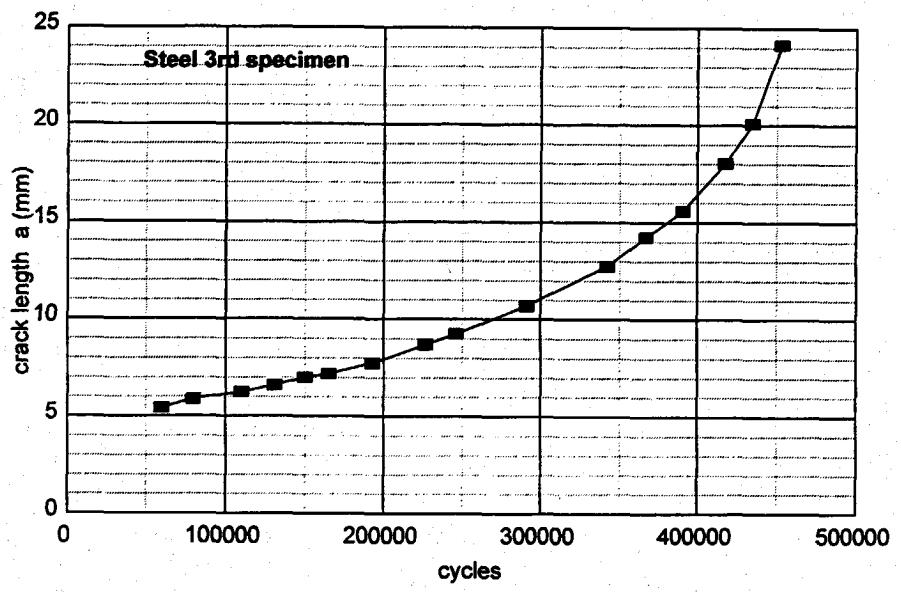

Fig.7a: Specimen Steel-3. Crack growth curve from records.

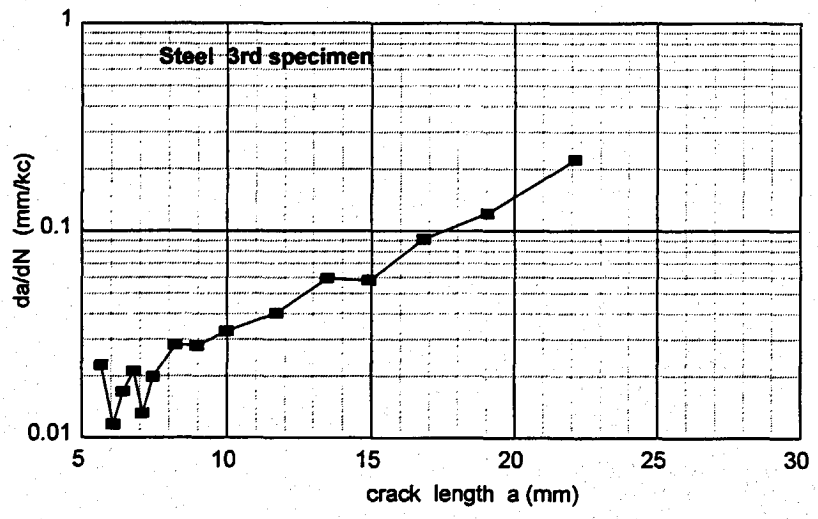

Fig.7b:
Specimen Steel-3.
Crack growth rates from records.

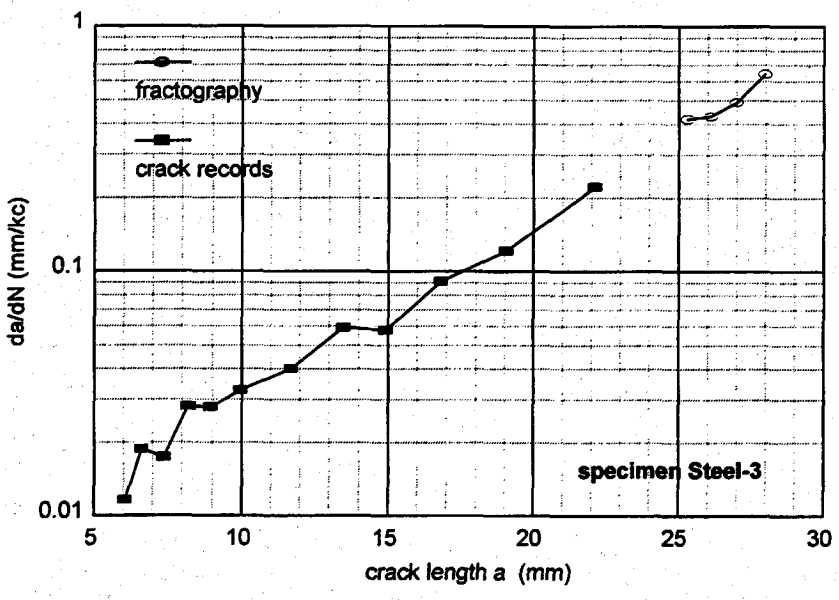

Fig.7c: Crack growth rates after omitting some data pairs (a,N). Fractographic results added.

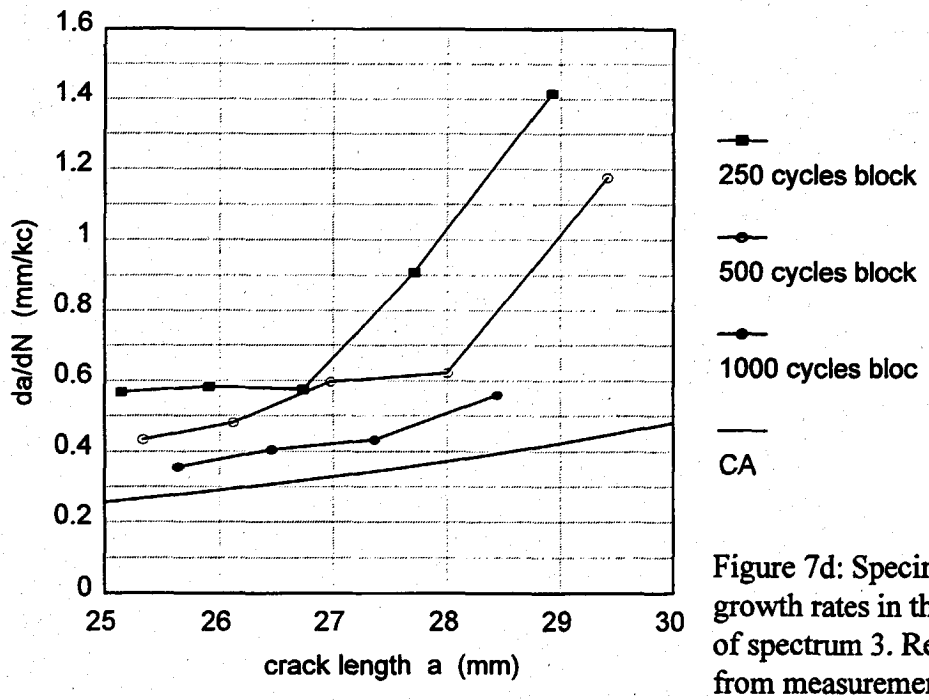

Figure 7d: Specimen Steel-3. Crack growth rates in the three sub-blocks of spectrum 3. Results obtained from measurements on fractographs.

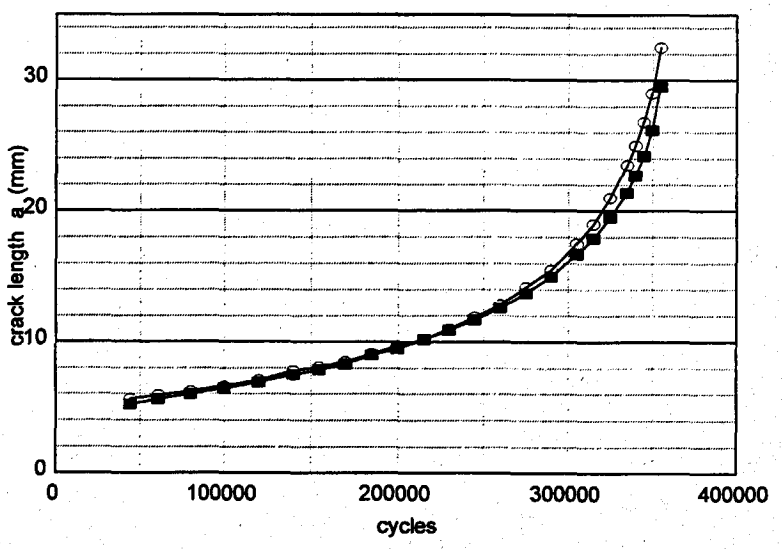

Fig.8a: Crack growth curve for left and right hand crack.

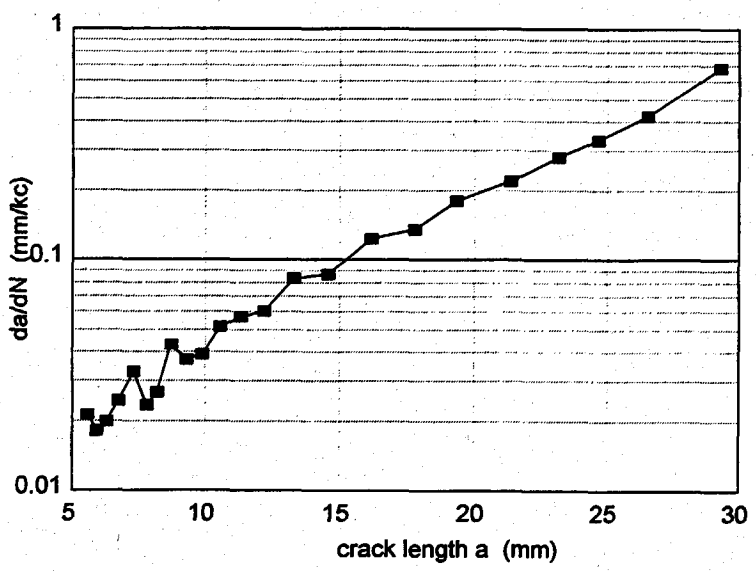

Fig.8b: Crack growth rate from records.

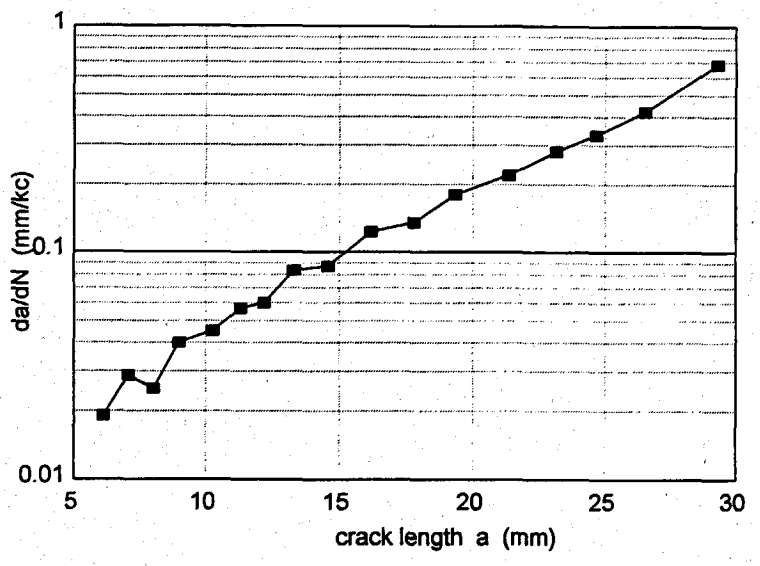

Fig.8c: Crack growth rates from streamlined data (leaving out some a,N data).

Fig.8: Specimen Steel-4 tested under CA loading.

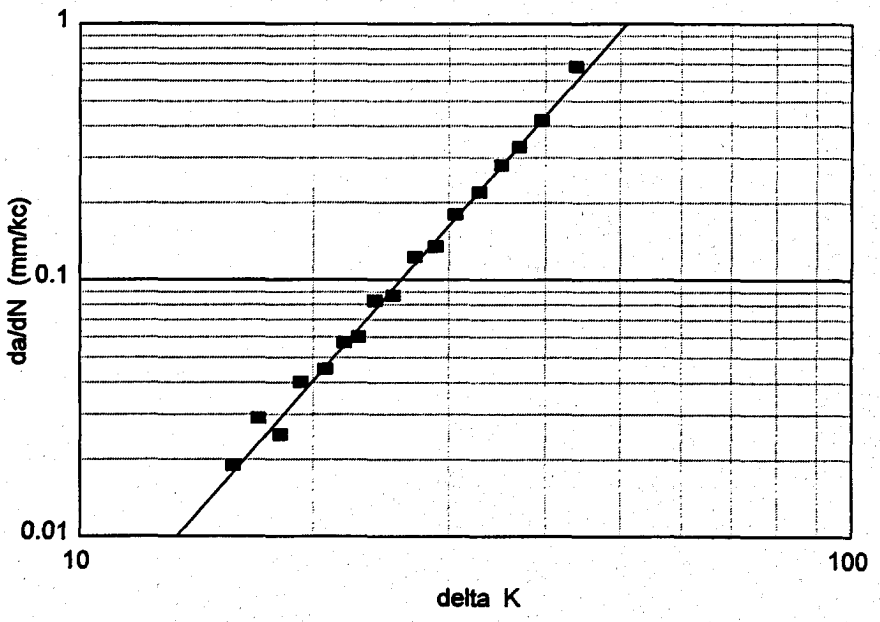

Figure 8d: CA crack growth rate results and the Paris relation, Eq.(1).

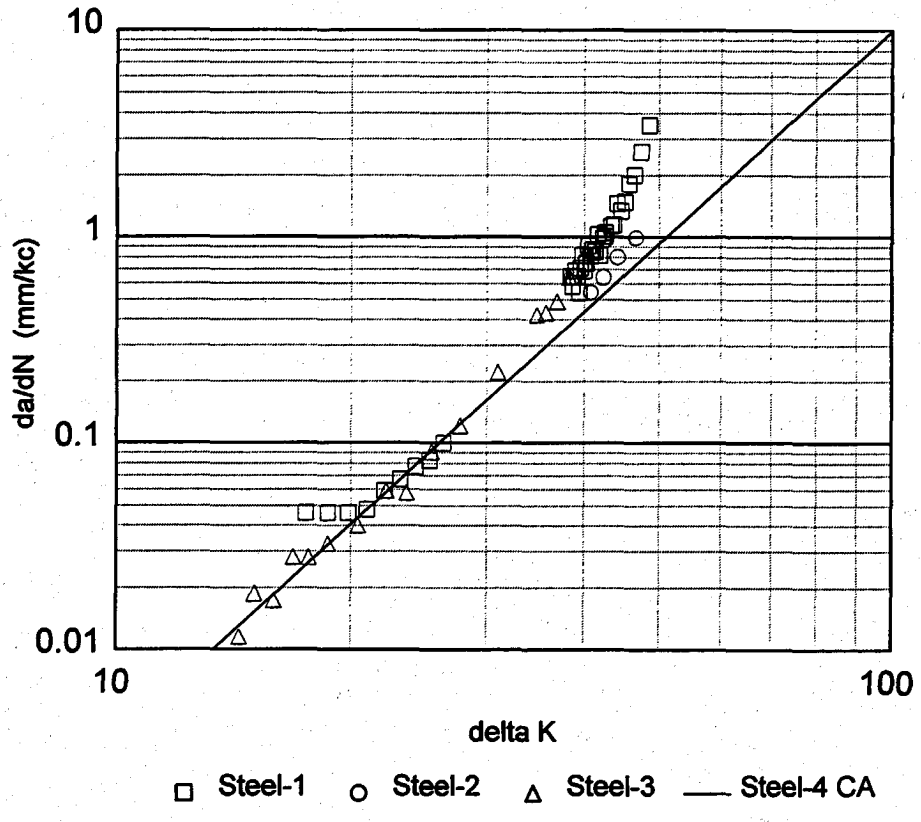

Figure 9: Comparison of the crack growth rates of the four specimens.

For specimens 1, 2 and 3 ΔK is calculated for the base line cycles.

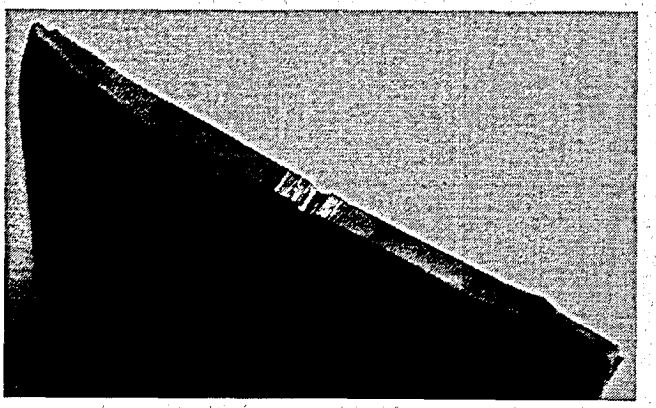

Fig.10a: Fracture surface of specimen.

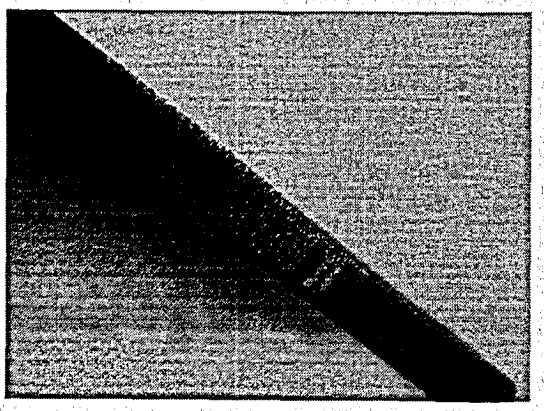

Fig.10b: Bands on fatigue fracture surface at larger values of the crack length.

Figure 10: Macro pictures of a failed fatigue specimen.

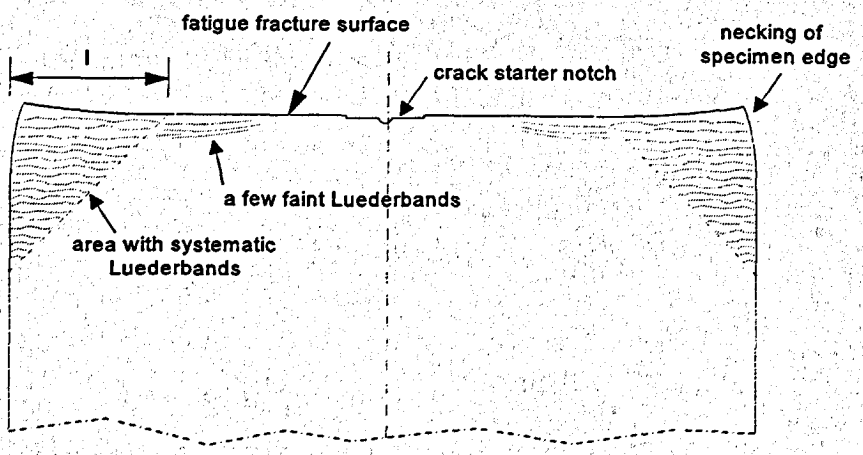

Fig.11: Lüderbands visible on polished surfaces of specimens Steel-3 and Steel-4.

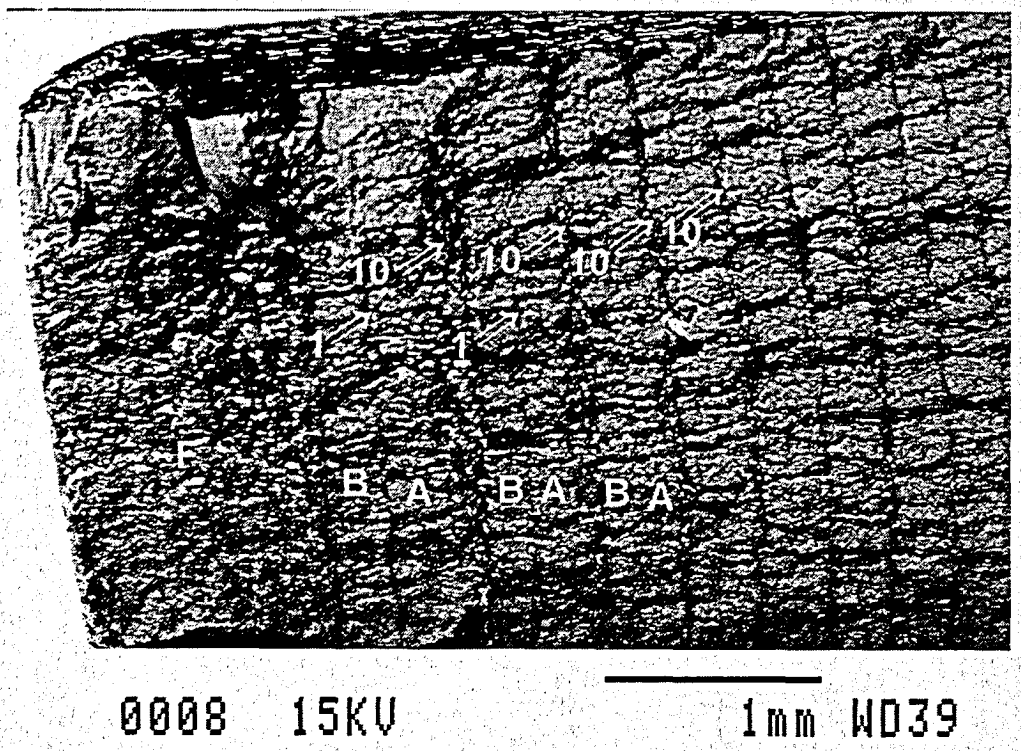

Fig.12: The last part of the fatigue crack of specimen Steel-1.
F = final failure
A = crack extension area of 100 base line cycles after the 10 OL's
B = crack extension area of 100 base line cycles after the single OL
Arrows 10 and 1 indicate the bands of the 10 OL cycles and the single OL respectively.

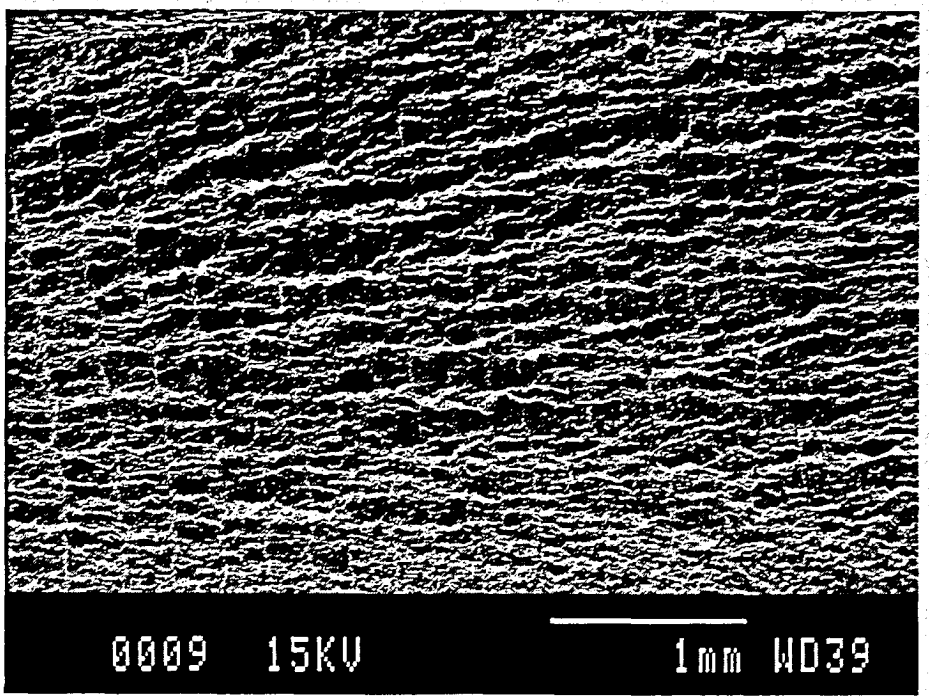

Fig.13: Bands of the 10 OL cycle batches of specimen Steel-1, from a≈25 to a≈29 mm. Bands of the single OL cycles can not be seen. Crack growth from right to left.

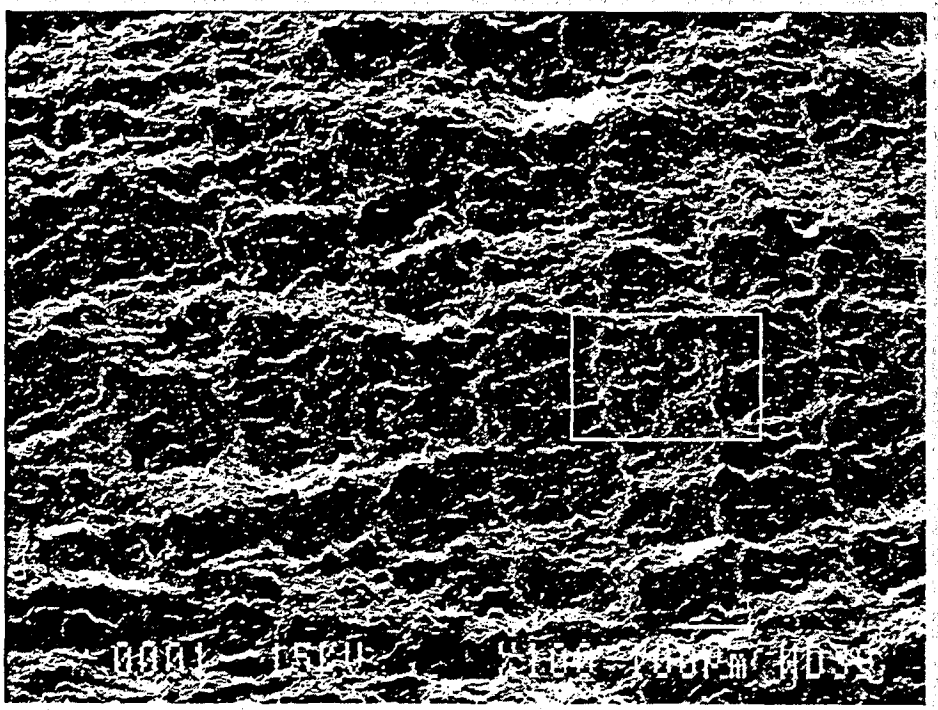

Fig.14: Magnification of detail of Fig.13. Bands of 10 OL cycles are visible, but bands of single OL cycle can hardly be observed.

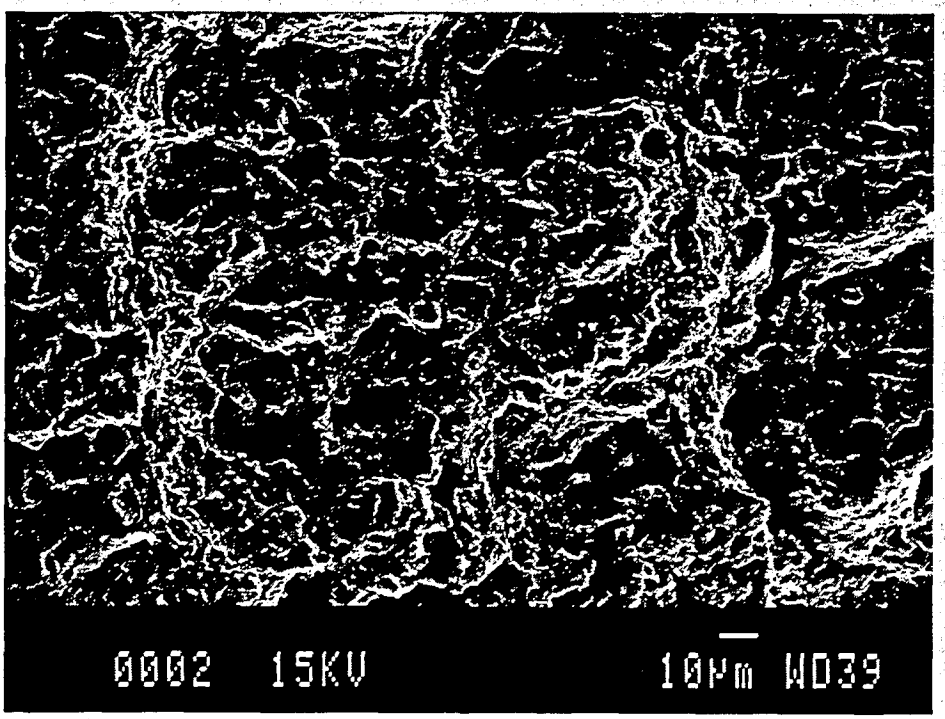

Fig.15: Detail of Fig.14 (white rectangular).

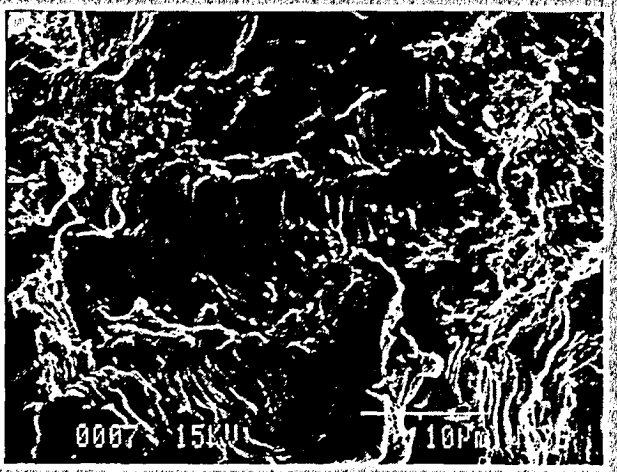

Fig.16: Specimen Steel-1.
Crack length a = 27.2 mm. Probably striations.
Crack rate according to Fig.5e ≈ 0.8 µm.

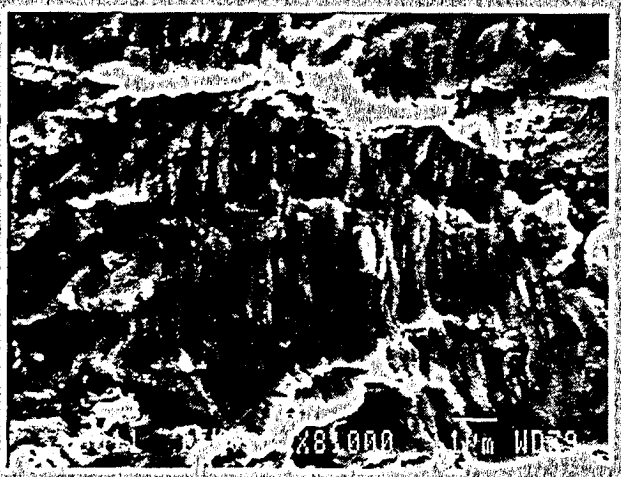

Fig.17: Specimen Steel-1.
Crack length a = 9.8 mm. Lines are probably not striations. Crack rate according to Fig.5d ≈0.045 µm/cycle.

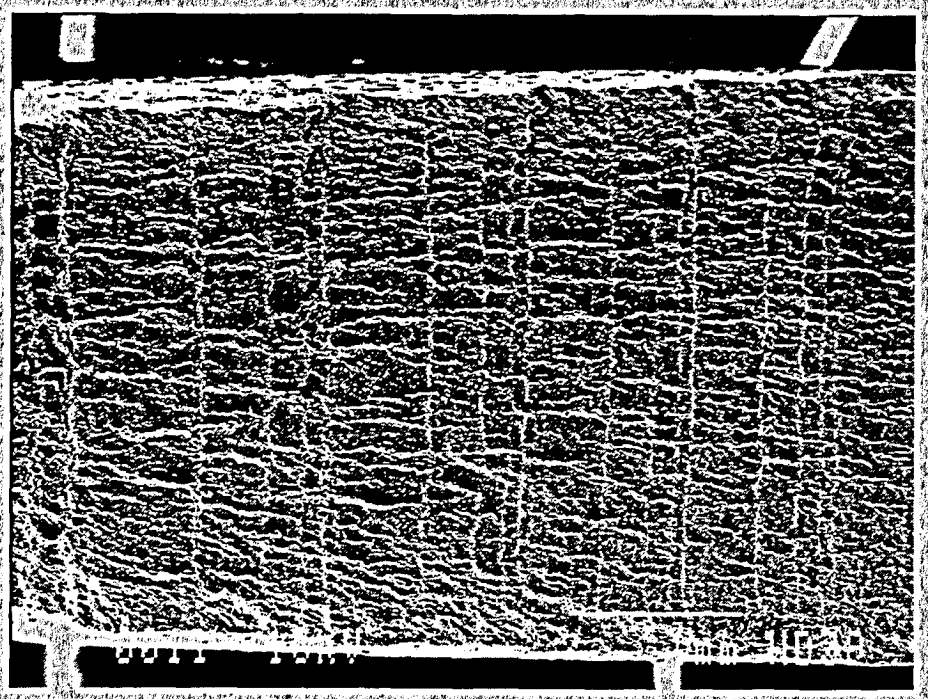

Fig.18: Specimen Steel-2. Four bands per period of load spectrum 2 clearly visible.
Crack growth from right to left, from a ≈ 26 mm to a ≈ 30 mm.

A, B, C, D correspond to blocks of 100, 200, 400, 800 small cycles respectively.

Fig.19: Picture made on band of a 20 OL cycles batch between 800 and 400 small cycles. Possibly striations of the OL cycles.

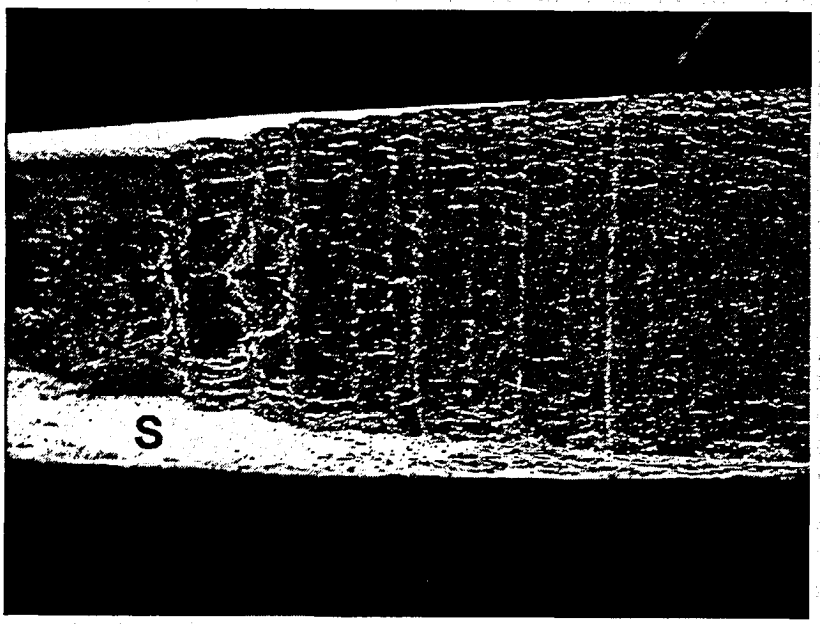

Fig.20: Specimen Steel-3. A, B, C correspond to the sub-blocks of 250, 500 and 1000 small cycles respectively. S = shear lip, F = final failure. The arrows indicate slag streaks at mid thickness.

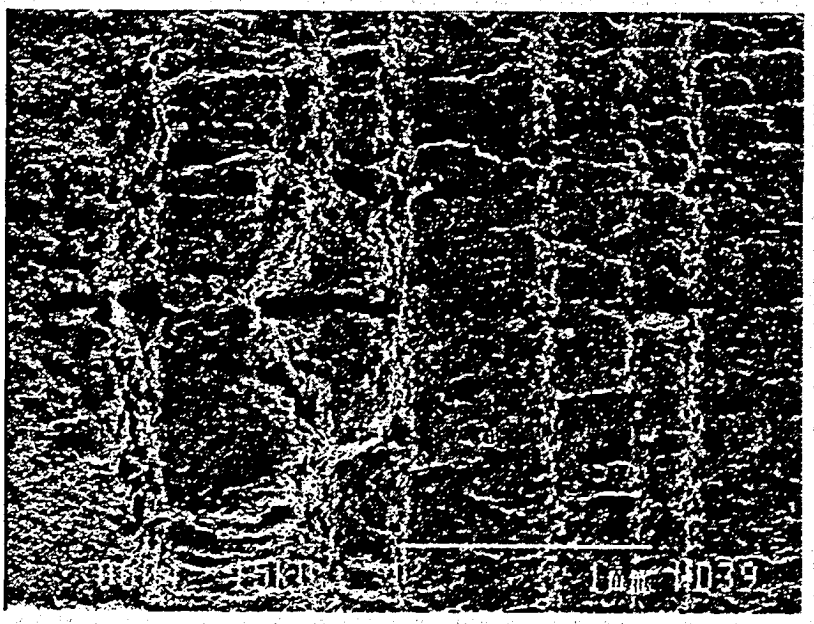

Fig.21:Detail of Figure 20.

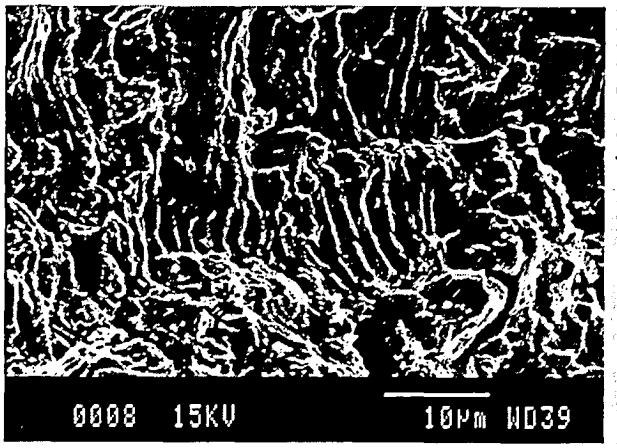

Fig.22: Specimen Steel-3, a = 27.4 mm. Picture of OL cycle band with striations of the OL cycles. Average striation spacing is $\Delta a \approx 1.5$ µm. The average crack growth rate at this crack length is about 0.5 µm/cycle (Fig.7c).

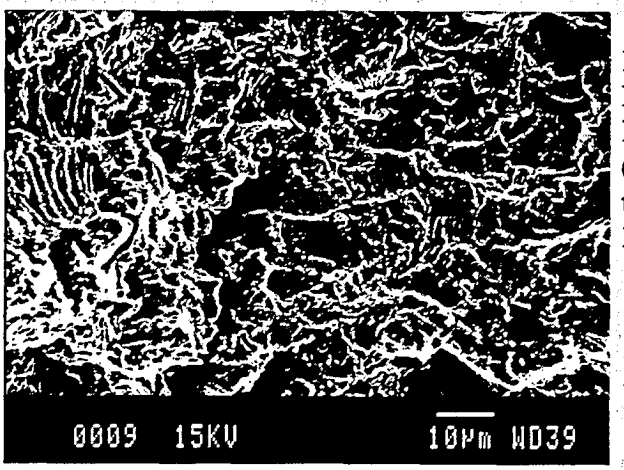

Fig.23: Specimen Steel-3, a = 27.4 mm. Picture at right hand side of OL striations of Fig.22. The two pictures are partly overlapping (notice different magnifications). Striations of the small cycles are visible in the middle and left hand part of this figure.

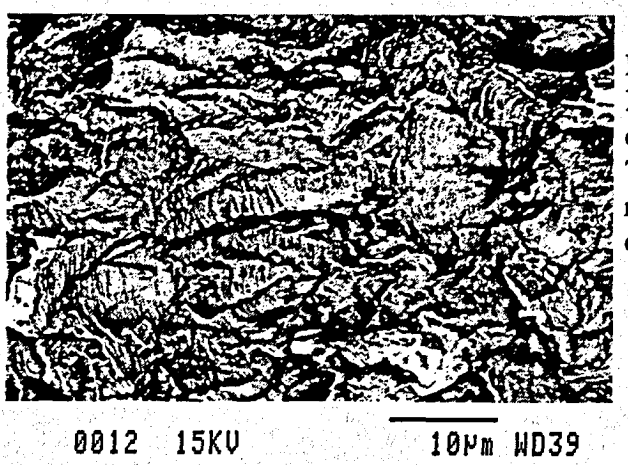

Fig.24: Specimen Steel-3, a = 15.7 mm. Faint striations are visible. Picture with inversed colors to enhance the visibility of the striations. The striation spacing is in the order of 0.5 µm, much smaller than the average crack rate at this crack length of $da/dN \approx 0.07$ µm/cycle (Fig.7c).